Distinct fiber-specific white matter reductions pattern in early- and late-onset Alzheimer's disease

Xiao Luo
The second affiliated hospital of Zhejiang University School of Medicine
Shuyue Wang
The second affiliated hospital of Zhejiang University School of Medicine
Yeerfan Jiaerken
The second affiliated hospital of Zhejiang University School of Medicine
Kaicheng Li
The second affiliated hospital of Zhejiang University School of Medicine
Qingze Zeng
The second affiliated hospital of Zhejiang University School of Medicine
Hui Hong
Zhejiang University School of Medicine
Xiaojun Guan
Zhejiang University School of Medicine
Tao Guo
Zhejiang University School of Medicine
Chao Wang
Zhejiang University School of Medicine
Ruiting Zhang
Zhejiang University School of Medicine
Jiong Zhou
Zhejiang University School of Medicine
Dan Wu
College of Biomedical Engineering and Instrument Science, Zhejiang University
Peiyu Huang
The second affiliated hospital of Zhejiang University School of Medicine
Minming Zhang (zhangminming@zju.edu.cn)
Department of Radiology, 2nd Affiliated Hospital of Zhejiang University

Research

Keywords: Alzheimer's disease, Early-onset Alzheimer's disease, Fixel-based analysis, diffusion tensor imaging, White matter

Posted Date: April 9th, 2020

DOI: https://doi.org/10.21203/rs.3.rs-21399/v1

Version of Record: A version of this preprint was published at Aging on April 30th, 2021. See the published version at https://doi.org/10.18632/aging.202702.

Abstract

Background Early-onset Alzheimer's disease (EOAD) has more domain cognitive deficits and worse prognosis than late-onset Alzheimer's disease (LOAD). However, changes to white matter fiber pathways subserving the structural networks are still unclear, mainly due to the difficulty of modeling crossing-fiber populations. Thus, we used the recently established method, fixel-based analysis (FBA), to investigate fiber-specific white matter (WM) reduction patterns in EOAD and LOAD.

Methods We identified 31 EOAD, 45 LOAD, 64 younger and 46 healthy elder controls (YHC/OHC). To repeat results, we further performed FBA in the ADNI database, including 17 EOAD, 30 LOAD, 31 YHC, and 34 OHC. Each subject underwent diffusion MRI scanning and neuropsychological assessments. Subjects from the ADNI database additionally underwent florbetapir and flortaucipir-PET examination. We measured the fiber density (FD) and fiber bundle cross-section (FC), then compared patients versus their counterparts (FWE corrected, $P < 0.05$). According to fixel-wise results, we further performed the tract of interest analyses.

Results In the ZJU database, EOAD had decreased FD in the splenium of CC (SCC), limbic tracts, cingulum bundles, and posterior thalamic radiation (PTR), and decreased FC in the SCC, dorsal cingulum and PTR. By contrast, LOAD had comparable FD and FC decrease, centered to the SCC, cingulum bundles, and posterior association tracts. Both EOAD and LOAD had a similar decrease in FDC, mainly involving the cingulum bundle. Importantly, we found similar trends in the ADNI database. Correlation results showed that both the FD and FC were related to multiple cognitive performance and disease severity. Further, FD of fornix column and body and FC of ventral cingulum correlated with composite amyloid ($r = -0.34$) and tau level ($r = -0.53$) reflected by PET imaging, respectively.

Conclusions Distinct WM damage in EOAD and LOAD might account for different cognitive pictures. Further, FD and FC might reflect different pathophysiological processes.

1. Background

Alzheimer's disease (AD) characterized by amyloid plaques and neurofibrillary tangles (NFTs) [1]. According to the onset age (65 years), we could further divide AD into early- and late-onset Alzheimer's disease (EOAD/LOAD) [2]. Not merely dementia occurring at a younger age, EOAD had a shorter survival time than LOAD, due to its more atypical clinical symptoms and faster clinical course [3]. Apart from memory deficit, EOAD also tends to have worse performance in attention, visuospatial skills, and executive functions [4, 5]. Both EOAD and LOAD share the same neuropathological hallmarks but present distinct deposition patterns [6, 7]. Topologically, multiple studies have reported that EOAD patients show higher burdens of amyloid deposition and NFTs than LOAD in frontal and parietal lobes [8–10].

Although core AD pathology mainly involves cortex, WM is not spared. Previous work diffusion tensor imaging (DTI) work demonstrated that LOAD has altered fractional anisotropy (FA) and mean diffusivity (MD) in the posterior cingulum, corpus callosum, and temporal lobes; while EOAD had more widespread

WM damage than LOAD [11]. Combined with the distinct cognitive profile of EOAD and LOAD, suggesting WM microstructure abnormalities serve as a useful imaging AD marker. Recently, the widely accepted disconnection hypothesis states that AD is featured by altered segmentation or integration relationships within or between intrinsic brain networks. Both the EOAD and LOAD have comparable changes in the default mode network (DMN), which is closely related to memory; but EOAD has more disruptions in networks relating to the executive, language, and visuospatial functions [12–14]. Considering the correlation between structural and functional connectivity, investigating alterations within specific WM pathways would provide a greater understanding of EOAD.

However, the major drawback of the diffusion model is its insufficient ability to model crossing-fiber populations [11]. Accordingly, a novel analytic framework known as fixel-based analysis (FBA) was proposed, which may improve the specificity for investigating WM changes by separating the WM damage in micro- and macrostructural level [15]. FBA metrics comprise the fiber density (FD) and cross-section (FC), represent the micro- and macrostructural properties of the fiber bundle, respectively. Considering the different WM damage patterns between EOAD and LOAD, we thus hypothesize that FBA may disentangle these alterations, improving our understanding of the neuropathological mechanism. Our study aims include: 1) assess fixel-specific WM damage pattern in EOAD and LOAD; 2) determine if these WM properties are associated with cognitive and neuropathological biomarkers; 3) validate result reproducibility in two independent databases.

2. Methods

2.1 Participant and neuropsychological assessment

Each participant underwent multi-sequence MRI scanning and comprehensive neuropsychological evolutions. In the ZJU database, the diagnosis of probable AD was made by an experienced neurologist according to the NINCDS/ADRDA criteria. Regarding the ADNI database (**Supplementary materials 1**), neurologists from multiple cooperation institutes made the AD diagnosis. Consistent with previous studies, we dichotomized AD patients into early- and late-onset groups (age at onset <65 or ≥ 65 years, respectively) [9, 11]. Detailed inclusion and exclusion criteria are available in **Supplementary materials 2**.

We grouped controls into younger and older healthy controls (YHC/OHC, age <65 or ≥ 65 years, respectively). The age, education, and sex of YHC and OHC matched well to their corresponding patient groups, respectively. Finally, 31 EOAD, 45 LOAD, 64 YHC, and 46 OHC from the ZJU database, as well as 17 EOAD, 30 LOAD, 31 YHC, and 34 OHC from the ADNI database were identified (**Table 1 and Supplementary Table 1)**.

2.2 MR imaging acquisition

In both databases, researchers used foam padding and earplugs to limit head motion and reduce scanner noise. Regarding the ZJU database, MRI data were acquired from the 3.0 Tesla scanner (GE Discover 750) using an 8-channel head coil. We acquired the T1-weighted structural images based on the fast-spoiled gradient-echo sequence with TR = 7.3 ms, TE = 3.0 ms; slice number = 196; FOV=256 ×256; voxel size=1.02 ×mm ×1.02 ×mm 1.2×mm; flip angle = 11°; and bandwidth = 244.141 Hz/pix. DWI data were acquired using a single shot, diffusion-weighted spin-echo echo-planar imaging sequence. Specifically, images were acquired using b = 1,000 s/mm^2 in 30 directions; 5 volumes were acquired without diffusion weighting (b-value = 0 s/mm^2). Other parameters of DTI were as follows: TR/TE = 8,000/80.8 ms, flip angle = 90°, slice thickness = 2 mm without slice gap, matrix size = 128 × 128, FOV = 256 × 256. More information of ADNI acquisition in Supplementary material 3.

2.3 DWI pre-processing and FBA

The DWI data pre-processing and FBA were performed using MRtrix3 (www.mrtrix.org) [16]. We firstly denoised the DWI and then corrected eddy-current, head motion, and bias field; then we normalized intensity across subjects. One experienced radiologist visually inspected the processed images.

Before the FBA, an average response function was firstly generated by averaging all subjects' single fiber response function. Then, fiber orientation distributions (FODs) were estimated using constrained spherical deconvolution (CSD), and we applied multi-shell multi-tissue (MSMT) CSD to obtain more robust outcomes [17]. From between-group comparisons, we generated a young subjects' FOD template based on randomly selected 10 EOAD and 10 YHC. Similarly, we calculated the elder subjects' FOD template. Then the fiber orientation distributions in the template were segmented to fixels for generating the fixel template analysis mask. For spatial correspondence, the FOD image of each subject was transformed into the corresponding template. Then we used resulting local transformations to segment and reorient fixels to match the template in each voxel. Finally, we assigned FD, FC, and FDC to fixels in the template space.

To facilitate connectivity-based fixel enhancement (CFE), whole-brain probabilistic tractography was performed on a group-wised FOD template. A total of 20 million streamlines was generated and filtered to 2 million for reducing reconstruction biases using the spherical deconvolution informed filtering of tractograms (SIFT) algorithm [18].

2.4 Tensor based analyses

Based on FSLo compare the result differences between the novel and conventional approaches, we performed the tract-based spatial statistics (TBSS) to re-evaluate the white matter degenerations in the ZJU database based on FSL (http://www.fmrib.ox.ac.uk/fsl/) [9, 10]. We calculated the commonly used metrics, fractional anisotropy (FA) and mean diffusivity (MD), then projected them to a target skeleton. Specially, (1) the FA template was selected as the target image; (2) the nonlinear transformation that mapped each subjects' FA to the target image computed using the FMRIB's non-linear image registration tool; (3) the same transformation was used to align each subject's FA to the standard space. A mean FA image was then created by averaging the aligned individual FA images and thinned to generate an FA skeleton representing WM tracts common to all subjects. After generating the FA skeleton, we then performed a voxel-wise comparison by using the threshold-free cluster enhancement to determine group differences between EOAD and YNC, as well as LOAD and ONC (Threshold-Free Cluster Enhancement, TFCE corrected, $p < 0.05$) [11].

2.5 PET image data

In the ADNI database, 13 out of 17 EOAD (76.5%), 27 out of 30 LOAD (90.0%), 12 out of 31 YHC (38.7%), and 32 out of 34 OHC (94.1%) had florbetapir PET data; 6 out of 17 EOAD (35.3%), 18 out of 31 YHC (58.1%), and 16 out of 34 OHC (47.0%) had flortaucipir-PET data [19]. Based on prior-defined regions of interest (ROI), standardized update value ratios (SUVRs) were calculated using the mean signal of the whole cerebellar (florbetapir) and cerebellar cortex (flortaucipir) as the reference region. We chose 4 ROI including the SUVRs of composite amyloid deposition and Tau from Braak stage I/II, III/IV, and V/VI (**Supplementary materials 2**) [1].

2.6 Statistical analysis

2.6.1 Analysis of demographics

Based on the SPSS (Statistical Product and Service Solutions, Version 23) of the Window system, we performed statistical analyses of demographic data. Continuous variables were compared using two-sample T-tests. Group differences in categorical variables were assessed using Fisher's exact test.

2.6.2 Fixel-based analysis

We first compared FD, FC, and FDC in the fixel level (FWE corrected, P-values < 0.05, 5000 permutations, controlling age and sex). We performed connectivity-based smoothing and statistical inference using CFE

(smoothing = 10 mm full-width at half-maximum, C = 0.5, E = 2, H = 3) [20]. Significant streamlines were color-coded by the effect size (percentage) relative to their corresponding controls.

2.6.3 Tract-based analysis and correlation analysis

Based on fixel-based analysis results, we focused on 12 tracts, including the splenium of corpus callosum (SCC), fornix column and body, bilateral dorsal and ventral cingulum, inferior longitudinal fasciculus/inferior frontal-occipital fasciculus (ILF/IFOF), posterior thalamic radiation (PTR), and fornix-hippocampus (HP). We extracted mean FD, FC, and FDC values from tracts and used two-sample t-tests to assess the differences of FBA metrics between AD patients and counterpart, controlling for age and sex (Bonferroni-corrected, P-value < 0.05). Furthermore, we explored the correlation between mean FBA metrics and cognitive performances, as well as PET biomarkers (P-value < 0.001 uncorrected, controlling for age and sex).

3. Results

3.1 Demographics

Patients and control groups did not significantly differ in age, gender, education. Further, for each database, no general cognitive score differences were found between EOAD and LOAD, as well as YHC and OHC ($p > 0.05$). Further, there is no interaction relationship between the effect of onset age (< 65 or ≥ 65 years) and disease status (healthy control or AD patients) ($p > 0.05$). Notably, patients in the ADNI database (**Supplementary Table 1**) had milder disease severity and higher education than those patients in the ZJU database (Table 1).

3.2 Whole-brain FBA results

3.2.1 ZJU database

EOAD had a widespread FD decrease in the SCC, fornix column and body, left fornix-HP, bilateral dorsal/ventral cingulum, and PTR; additionally, EOAD had FC decrease in the SCC, bilateral dorsal cingulum, and PTR. Regarding the composite index, EOAD had a widespread FDC decrease in the SCC, left fornix-HP, bilateral dorsal/ventral cingulum, and PTR relative to YHC. By contrast, we found that LOAD patients had an FD decrease in the bilateral dorsal/ventral cingulum and left ILF/IFOF and had an FC decrease in the SCC, bilateral dorsal/ventral cingulum, PTR, and ILF/IFOF relative to OHC. Further, LOAD had decreased FDC in the SCC, bilateral dorsal/ventral cingulum, ILF/IFOF, and PTR (Fig. 1, **left**).

3.2.2 ADNI database

EOAD had decreased FD in the whole CC, fornix column and body, and left ventral cingulum compared to YHC, but no FC difference between EOAD and YHC existed. EOAD only had FDC decreases in the left ventral cingulum. By contrast, LOAD had an FD decrease in the SCC, fornix column and body, right fornix HP, and left ventral cingulum relative to OHC. Further, LOAD had decreased FC in the fornix column and body and left dorsal cingulum, and FDC decreases in the SCC and left dorsal/ventral cingulum (Fig. 1, **right**).

3.3 Tract level analysis

3.3.1 ZJU database

EOAD had decreased mean FD in the SCC, fornix column and body, bilateral dorsal/ventral cingulum, right PTR, left fornix-HP, as well as decreased mean FC in the SCC, bilateral dorsal cingulum and PTR; further, EOAD had mean FDC decrease in the SCC, bilateral cingulum bundles and PTR, and left fornix-HP. On the other side, LOAD had decreased mean FD in the right dorsal cingulum, bilateral ventral cingulum, left ILF/IFOF, as well as decreased mean FC in the SCC, bilateral ILF/IFOF and PTR. Additionally, LOAD exhibited mean FDC decreases in the SCC, bilateral cingulum bundles, ILF/IFOF, and PTR (Fig. 2).

3.3.2 ADNI database

EOAD had decreased mean FD in the fornix column and body and left ventral cingulum. However, no difference in mean FC and FDC between EOAD and YHC existed. On the other side, LOAD had significantly decreased mean FD in the fornix column and body, bilateral ventral cingulum, as well as decreased mean FC in the fornix column and body. Further, LOAD patients had decreased FDC in left cingulum HP.

3.4 Relationship between fixel-based metrics and cognitive/neuropathologies

Across four groups (EOAD, YHC, LOAD, and OHC), we correlated both the mean FD and FC with the cognitive score. Concisely, we only displayed the correlation results between mean FBA metrics (i.e., FD and FC) and MMSE/CDR sum (**Supplementary Materials 6/7)**. Further, within the ADNI database, we correlated both the mean FD and FC with PET-derived AD neuropathological markers.

3.4.1 ZJU database

We found that MMSE was related with FD in the SCC (r = 0.33), bilateral dorsal cingulum (r = 0.40/0.38, respectively), left ventral cingulum (r = 0.48), bilateral ILF/IFOF (r = 0.23/0.25, respectively); while CDR sum was related with FD in the SCC (r = -0.31), bilateral dorsal cingulum (r = -0.28/-0.26, respectively), left ventral cingulum (r = -0.42). On the other side, we found that MMSE was related with FC in the SCC (r = -0.35), bilateral dorsal cingulum (r = 0.26/0.33, respectively), ILF/IFOF (r = 0.28/0.25, respectively), and

PTR (r = 0.39/0.43, respectively); while CDR sum was related with FC in the SCC (r = -0.29), left dorsal cingulum (r = -0.28), and bilateral PTR (r = -0.32/-0.35, respectively).

3.4.2 ADNI database

We found that MMSE was related with FD in the SCC (r = 0.33), bilateral dorsal cingulum (r = 0.40/0.38, respectively), left ventral cingulum (r = 0.48), and bilateral ILF/IFOF (r = 0.23/0.25, respectively); while CDR sum was related with FD in SCC (r = -0.31), bilateral dorsal cingulum (r = -0.28/-0.26, respectively), left ventral cingulum (r = 0.42). On the other side, MMSE was related with FC in the SCC (r = 0.35), bilateral dorsal cingulum (r = 0.26/0.33, respectively), ILF/IFOF (r = 0.28/0.25, respectively), PTR (r = 0.39/0.43, respectively); while CDR sum was related with FC in the SCC (r = -0.29), left dorsal cingulum (r = -0.28), and bilateral PTR (r = -0.32/-0.35, respectively).

3.4.3 Association between FBA metrics and PET data

Across groups in the ADNI database, FD of fornix column and body correlated with composite amyloid deposition SUVR (r = -0.34), while right ventral cingulum FC correlated with mean tau retention of Braak I-II ROI, including the bilateral entorhinal and hippocampus (r = -0.53).

3.5 Repeated analyses after matching sample size of two databases

To eliminate the differences potentially caused by statistical effects, we matched the sample size of two databases by reducing the subjects in the ZJU database. However, results were mostly unchanged (**Supplementary materials 5**).

4. Discussion

The main findings include: (i) WM damage is more widespread in EOAD, but more pronounced and restricted in LOAD; (ii) in both databases, EOAD is featured by FD decrease rather than FC; (iii) FD and FC were related to cognitive, disease severity, and different pathological markers. Therefore distinct WM damage pattern between EOAD and LOAD account for different cognitive pictures and pathological processes.

4.1 WM damage is more widespread in EOAD, but more pronounced and restricted in LOAD

WM damage in LOAD was centered on the bilateral dorsal and ventral cingulum and ILF/IFOF across two databases. Notably, WM impairments of LOAD were more pronounced, though less spatially extensive than EOAD. This result is consistent with the evidence that AD patients with a younger onset age had less pathology in the hippocampus but extensive involvement of cortex [21]. Anatomically, the cingulum bundle connects the anterior medial prefrontal cortex, PCC, and medial temporal lobe, which are the core regions of DMN [22]. Besides, bilateral ILF/IFOF directly connect angular gyrus with DMN [23]. Our results

thus suggested that WM tracts subserving DMN are especially susceptible to damage effects. Similarly, previous functional studies also reported that LOAD patients were featured by restricted DMN disconnection [12–14]. Our TBSS results also showed that LOAD had a more extensive FA decreased or MD increased than both the results of FD or FC (**Supplementary materials 4**).

Importantly, EOAD exhibited additional WM damage in the fornix column and body, left fornix-HP, SCC, and PTR. Previous work also demonstrated that EOAD had more widespread WM microstructural damage than LOAD [11, 24]. Our WM results are also supported by previous functional imaging evidence, documenting that EOAD is featured by various network dysfunction involving executive control, visuospatial, language, and memory-related networks [12–14]. In detail, fornix-related tracts, as the structural support of DMN, lie along the HP concavity and prolonged into the parahippocampal gyrus; SCC accounts for the homotopic connections between the bilateral parietal and posterior cingulate cortices, comprising the executive-related network [25]; while PTR connects the thalamus with the visual cortex, acting as the foundation of visuospatial and language function [26]. Combined with correlation results that mean FBA metrics of fornix-related tracts, SCC, and PTR are related to multi-domain cognitive performance, we thus inferred that widespread WM loss in EOAD might contribute to cognitive deficits.

4.2 WM damage of EOAD is featured by reduced FD

In the ZJU database, EOAD showed a decrease in both FD and FC, while FC decrease was more salient than FD in LOAD. Decreased FD represents decreased volume fraction of restricted water within a voxel; while decreased FC reflects a shrink of fiber bundle's cross-sectional area [15]. FD and FC decrease thus might represent two pathological types. Therefore, EOAD may undergo WM disruption resulting from the damage effects of amyloid plaques and NFTs; By contrast, NFTs may dominate WM damages in LOAD. Our hypothesis is supported by results that FD and FC were associated with amyloid deposition and tau retention, respectively. Our interpretation in line with neuropathological results, documenting that EOAD had a higher burden of AD neuropathologies than LOAD. Additionally, in both EOAD and LOAD, we noted that WM tracts showing FD decreases (i.e., fornix-related tracts) were anatomically connected with DMN, which is the earliest region involved in amyloid pathologies. By contrast, tracts showing FC decrease are long projection fibers (e.g., PTR) from posterior cortices. This is consistent with the work showed that parietal WM damage in AD was driven more by NFTs than amyloid plaques [27].

4.3 Discrepant results between databases

Although most results showed same trend, still discrepancies existed between databases, even matching the sample size of two databases. In the ADNI database, damage range of FD and FC is smaller than ZJU. Additionally, patients of LOAD in ADNI manifested as salient FD decrease rather than FC, and vice versa for ZJU. Several reasons may account for the differences: first the clinical severity for the ADNI patients is milder than ZJU patients. Accordingly, WM tracts involved early in the AD continuum had similar damage degrees across databases, such as cingulum bundles and fornix-related tracts [28]. Second, brain reserve may alleviate WM damage, reflecting by microstructural WM damage first followed by macrostructural one [29]. Significantly, ADNI subjects had a higher education than ZJU.

Regarding limitations, first, based on the 2018 AD research framework, ATN biological diagnosis criteria are recommended to diagnose AD patients. Second, although the lower b-value should not influence the FC metric, higher b-value (3000s/mm^2) could improve the capability to resolve crossing fiber regions [15]. Conclusively, EOAD had more widespread WM microstructural damage than LOAD, which may contribute to worse cognitive profiles. Additionally, FD and FC could reflect different pathologies of WM loss.

5. Conclusion

We investigate the WM damage pattern difference between EOAD and LOAD. We found that EOAD had more widespread WM microstructural damage than LOAD, which may contribute to their worse cognitive profiles. WM microstructural and macrostructural damage was respectively associated with amyloid and NFTs, implicating that EOAD patients' WM are more susceptible to amyloid deposition.

6. List Of Abbreviations

FD, fiber density; FC, fiber bundle cross-section; FDC, fiber density & bundle cross-section; EOAD, early-onset Alzheimer's disease (EOAD); LOAD, late-onset Alzheimer's disease; YHC, young healthy controls, and OHC, old healthy controls

7. Declarations

7.1 Ethics approval and consent to participate

Regarding the ZJU database, our study was approved by the Review Board of the Second Affiliated Hospital, Zhejiang University School of Medicine, and conducted following the Declaration of Helsinki. We obtained the written informed consent from all participants. Regarding the ADNI database, this project was approved by the Institutional Review Boards of all participating institutions, and all of the participating institutions, and informed written consent was obtained from all participants at each site. More information could be found in http://adni.loni.usc.edu/.

7.2 Funding

This study was funded by the National Key Research and Development Program of China (NO.2016YFC1306600) and the National Natural Science Foundation of China (Grant No. 81901707). Data collection and sharing for our work was also supported by the Alzheimer's Disease Neuroimaging Initiative (ADNI) (National Institutes of Health Grant U01 AG024904) and DOD ADNI (Department of Defense award number W81XWH-12-2-0012).

7.3 Availability of data and materials

The ZJU database used and analyzed during the present study are available from the corresponding author on reasonable request. The ADNI is a longitudinal multicenter and open-source study, designed to develop clinical, imaging, genetic, and biochemical biomarkers for the early detection and tracking of AD.

7.4 Authors' contributions

Xiao Luo and Shuyue Wang designed the study and writing work. Peiyu Huang and MM Zhang contributed to data analysis and draft modification. YJ , KCL, QZZ, HH, XJG, TG, CW, RTZ, JZ, DW, Peiyu Huang contributed to the data collection and discussion. All authors read and approved the final manuscript.

7.5 Acknowledgement

None

7.6 Consent for publication

Not applicable.

7.7 Competing interests

The authors declare that they have no competing interests.

7.8 Author details

[1]Department of Radiology, The 2nd Affiliated Hospital of Zhejiang University School of Medicine, Hangzhou, China; [2]Department of Neurology, The 2nd Affiliated Hospital of Zhejiang University School of Medicine, Hangzhou, China; [3]Key Laboratory for Biomedical Engineering of Ministry of Education, College of Biomedical Engineering and Instrument Science, Zhejiang University, Hangzhou, China.

8. References

1. Braak H, Braak E: **Neuropathological stageing of Alzheimer-related changes**. *Acta neuropathologica* 1991, **82**(4):239-259.
2. Renvoize E, Hanson M, Dale M: **Prevalence and causes of young onset dementia in an English health district**. *International journal of geriatric psychiatry* 2011, **26**(1):106-107.
3. Koedam EL, Pijnenburg YA, Deeg DJ, Baak MM, Van Der Vlies AE, Scheltens P, Van Der Flier WM: **Early-onset dementia is associated with higher mortality**. *Dementia and geriatric cognitive disorders* 2008, **26**(2):147-152.

4. Smits LL, Pijnenburg YA, Koedam EL, van der Vlies AE, Reuling IE, Koene T, Teunissen CE, Scheltens P, van der Flier WM: **Early onset Alzheimer's disease is associated with a distinct neuropsychological profile**. *Journal of Alzheimer's Disease* 2012, **30**(1):101-108.
5. Joubert S, Gour N, Guedj E, Didic M, Guériot C, Koric L, Ranjeva J-P, Felician O, Guye M, Ceccaldi M: **Early-onset and late-onset Alzheimer's disease are associated with distinct patterns of memory impairment**. *Cortex* 2016, **74**:217-232.
6. Schöll M, Ossenkoppele R, Strandberg O, Palmqvist S, study SB, Jögi J, Ohlsson T, Smith R, Hansson O: **Distinct 18F-AV-1451 tau PET retention patterns in early-and late-onset Alzheimer's disease**. *Brain* 2017, **140**(9):2286-2294.
7. Cho H, Seo SW, Kim J-H, Suh MK, Lee J-H, Choe YS, Lee K-H, Kim JS, Kim GH, Noh Y: **Amyloid deposition in early onset versus late onset Alzheimer's disease**. *Journal of Alzheimer's Disease* 2013, **35**(4):813-821.
8. Choo IH, Lee DY, Kim JW, Seo EH, Lee DS, Kim YK, Kim SG, Park SY, Woo JI, Yoon EJ: **Relationship of amyloid-beta burden with age-at-onset in Alzheimer disease**. *The American Journal of Geriatric Psychiatry* 2011, **19**(7):627-634.
9. Cho H, Choi JY, Lee SH, Lee JH, Choi Y-C, Ryu YH, Lee MS, Lyoo CH: **Excessive tau accumulation in the parieto-occipital cortex characterizes early-onset Alzheimer's disease**. *Neurobiology of aging* 2017, **53**:103-111.
10. Ossenkoppele R, Zwan MD, Tolboom N, van Assema DM, Adriaanse SF, Kloet RW, Boellaard R, Windhorst AD, Barkhof F, Lammertsma AA: **Amyloid burden and metabolic function in early-onset Alzheimer's disease: parietal lobe involvement**. *Brain* 2012, **135**(7):2115-2125.
11. Canu E, Agosta F, Spinelli EG, Magnani G, Marcone A, Scola E, Falautano M, Comi G, Falini A, Filippi M: **White matter microstructural damage in Alzheimer's disease at different ages of onset**. *Neurobiology of aging* 2013, **34**(10):2331-2340.
12. Adriaanse SM, Binnewijzend MA, Ossenkoppele R, Tijms BM, van der Flier WM, Koene T, Smits LL, Wink AM, Scheltens P, van Berckel BN: **Widespread disruption of functional brain organization in early-onset Alzheimer's disease**. *PloS one* 2014, **9**(7):e102995.
13. Gour N, Felician O, Didic M, Koric L, Gueriot C, Chanoine V, Confort-Gouny S, Guye M, Ceccaldi M, Ranjeva JP: **Functional connectivity changes differ in early and late-onset alzheimer's disease**. *Human brain mapping* 2014, **35**(7):2978-2994.
14. Lehmann M, Madison C, Ghosh PM, Miller ZA, Greicius MD, Kramer JH, Coppola G, Miller BL, Jagust WJ, Gorno-Tempini ML: **Loss of functional connectivity is greater outside the default mode network in nonfamilial early-onset Alzheimer's disease variants**. *Neurobiology of aging* 2015, **36**(10):2678-2686.
15. Raffelt DA, Tournier J-D, Smith RE, Vaughan DN, Jackson G, Ridgway GR, Connelly A: **Investigating white matter fibre density and morphology using fixel-based analysis**. *Neuroimage* 2017, **144**:58-73.
16. Tournier J-D, Smith R, Raffelt D, Tabbara R, Dhollander T, Pietsch M, Christiaens D, Jeurissen B, Yeh C-H, Connelly A: **MRtrix3: A fast, flexible and open software framework for medical image processing**

and visualisation. *NeuroImage* 2019:116137.

17. Dhollander T, Connelly A: **A novel iterative approach to reap the benefits of multi-tissue CSD from just single-shell (+ b= 0) diffusion MRI data**. In: *Proc ISMRM: 2016*; 2016: 3010.
18. Smith RE, Tournier J-D, Calamante F, Connelly A: **SIFT: spherical-deconvolution informed filtering of tractograms**. *Neuroimage* 2013, **67**:298-312.
19. Landau SM, Lu M, Joshi AD, Pontecorvo M, Mintun MA, Trojanowski JQ, Shaw LM, Jagust WJ, Initiative AsDN: **Comparing positron emission tomography imaging and cerebrospinal fluid measurements of β-amyloid**. *Annals of neurology* 2013, **74**(6):826-836.
20. Raffelt DA, Smith RE, Ridgway GR, Tournier J-D, Vaughan DN, Rose S, Henderson R, Connelly A: **Connectivity-based fixel enhancement: Whole-brain statistical analysis of diffusion MRI measures in the presence of crossing fibres**. *Neuroimage* 2015, **117**:40-55.
21. Murray ME, Graff-Radford NR, Ross OA, Petersen RC, Duara R, Dickson DW: **Neuropathologically defined subtypes of Alzheimer's disease with distinct clinical characteristics: a retrospective study**. *The Lancet Neurology* 2011, **10**(9):785-796.
22. Greicius MD, Supekar K, Menon V, Dougherty RF: **Resting-state functional connectivity reflects structural connectivity in the default mode network**. *Cerebral cortex* 2009, **19**(1):72-78.
23. Hau J, Sarubbo S, Perchey G, Crivello F, Zago L, Mellet E, Jobard G, Joliot M, Mazoyer BM, Tzourio-Mazoyer N: **Cortical terminations of the inferior fronto-occipital and uncinate fasciculi: anatomical stem-based virtual dissection**. *Frontiers in neuroanatomy* 2016, **10**:58.
24. Li K-C, Luo X, Zeng Q-Z, Xu X-J, Huang P-Y, Shen Z-J, Xu J-J, Zhou J, Zhang M-M: **Distinct Patterns of Interhemispheric Connectivity in Patients With Early-and Late-Onset Alzheimer's Disease**. *Frontiers in aging neuroscience* 2018, **10**:261.
25. Jokinen H, Ryberg C, Kalska H, Ylikoski R, Rostrup E, Stegmann MB, Waldemar G, Madureira S, Ferro JM, van Straaten EC: **Corpus callosum atrophy is associated with mental slowing and executive deficits in subjects with age-related white matter hyperintensities: the LADIS Study**. *Journal of Neurology, Neurosurgery & Psychiatry* 2007, **78**(5):491-496.
26. Menegaux A, Meng C, Neitzel J, Bäuml JG, Müller HJ, Bartmann P, Wolke D, Wohlschläger AM, Finke K, Sorg C: **Impaired visual short-term memory capacity is distinctively associated with structural connectivity of the posterior thalamic radiation and the splenium of the corpus callosum in preterm-born adults**. *NeuroImage* 2017, **150**:68-76.
27. McAleese KE, Firbank M, Dey M, Colloby SJ, Walker L, Johnson M, Beverley JR, Taylor JP, Thomas AJ, O'Brien JT: **Cortical tau load is associated with white matter hyperintensities**. *Acta neuropathologica communications* 2015, **3**(1):60.
28. Mielke MM, Okonkwo OC, Oishi K, Mori S, Tighe S, Miller MI, Ceritoglu C, Brown T, Albert M, Lyketsos CG: **Fornix integrity and hippocampal volume predict memory decline and progression to Alzheimer's disease**. *Alzheimer's & Dementia* 2012, **8**(2):105-113.
29. Stern Y, Arenaza-Urquijo EM, Bartrés-Faz D, Belleville S, Cantilon M, Chetelat G, Ewers M, Franzmeier N, Kempermann G, Kremen WS: **Whitepaper: Defining and investigating cognitive reserve, brain**

reserve, and brain maintenance. *Alzheimer's & Dementia* 2018.

Table 1

Table 1. Clinical and demographic data of the ZJU database

Groups	YHC	EOAD	OHC	LOAD	Interaction		ANOVA	
					F/χ2	P-value	F/χ2	P-value
Number	64	31	46	45	/	/	/	/
Age, years	59.7 (2.5)	60.8 (3.3)	72.4 (3.8)	74.3 (4.6)	0.7	0.4	86.9	<0.001
Education, years	10.7 (3.7)	9.4 (2.9)	10.5 (4.1)	10.5 (4.0)	2.6	0.1	0.9	0.4
Sex, F/M	38/26	21/10	22/24	23/22	0.1	0.8	3.7	0.3
GDS	1.9 (2.5)	1.6 (1.5)	1.2 (1.6)	1.4 (1.2	0.7	0.4	1.2	0.3
Disease severity								
CDR global	0 (0)	1.1 (0.3)	0 (0)	1.0 (0.5)	0.2	0.6	220.9	<0.001
CDR sum	0 (0)	4.9 (2.1)	0 (0.1)	4.7 (3.6)	0.1	0.7	87.0	<0.001
General cognitive								
MMSE	28.1 (1.6)	20.6 (3.6)	28.3 (1.5)	20.0 (3.7)	0.7	0.4	140.0	<0.001
Memory								
LM delay	8.5 (4.3)	0.6 (1.3)	8.6 (3.7)	0.3 (0.7)	0.01	0.9	96.0	<0.001
Executive								
TMT-B	172.6 (64.3)	223.6 (90.6)	181.5 (69.8)	250.3 (83.4)	0.1	0.7	17.8	<0.001
Language								
SVF	16.3 (3.9)	11.0 (5.3)	16.0 (4.8)	8.9 (5.0)	3.6	0.1	31.3	<0.001
Attention								
TMT-A	69.2 (28.2)	98.3 (40.6)	70.8 (29.8)	106.3 (38.0)	0.4	0.6	16.5	<0.001
Visuospatial								
CDT	4.1 (0.7)	3.2 (0.6)	4.3 (0.6)	3.3 (0.6)	0.2	0.7	33.6	<0.001

 and represent the significant difference between YHC and OHC, as well as EOAD and LOAD ($p<0.05$), respectively. Interactive effects comprise the factors of onset age (<65 or ≥65 years) and disease status (controls or patients). Abbreviations: YHC, young healthy controls; EOAD, early-onset Alzheimer's disease; OHC, old healthy controls; LOAD, late-onset Alzheimer's disease; CDR global/sum, Clinical Dementia Rating, global score and sum score of box; MMSE, Mini-Mental State Examination; GDS, Geriatric Depression Scale; LM, Logical Memory; TMT-A/B, Trail Making Test, part A/B; SVF, Semantic Verbal Fluency

Figures

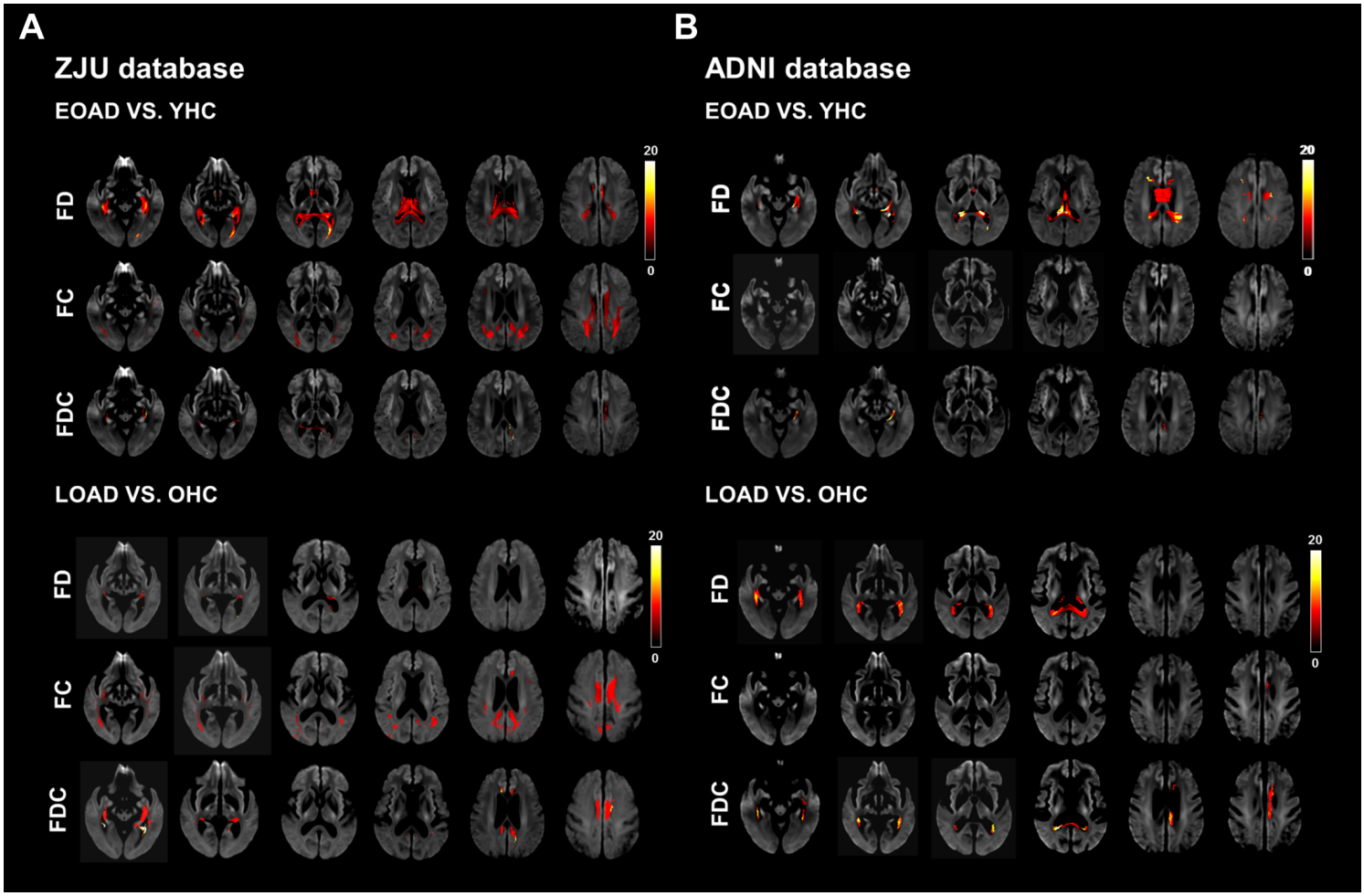

Figure 1

illustrates the location reference and fiber tract-specific reduction in EOAD/LOAD versus controls from whole-brain FBA.

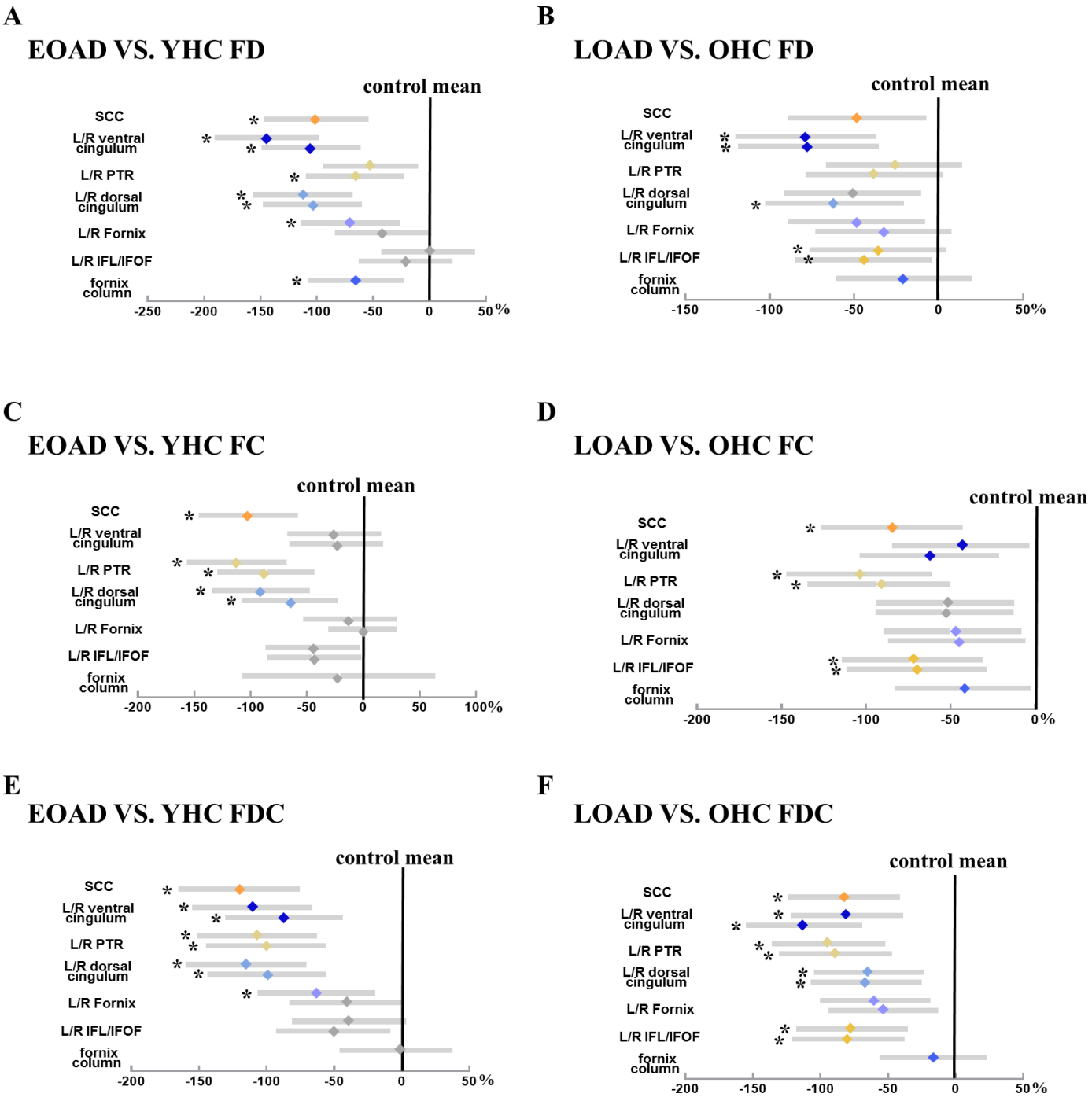

Figure 2

illustrates the group difference (patient VS. control) in mean fiber density and cross-section (FDC) based on the ZJU database.

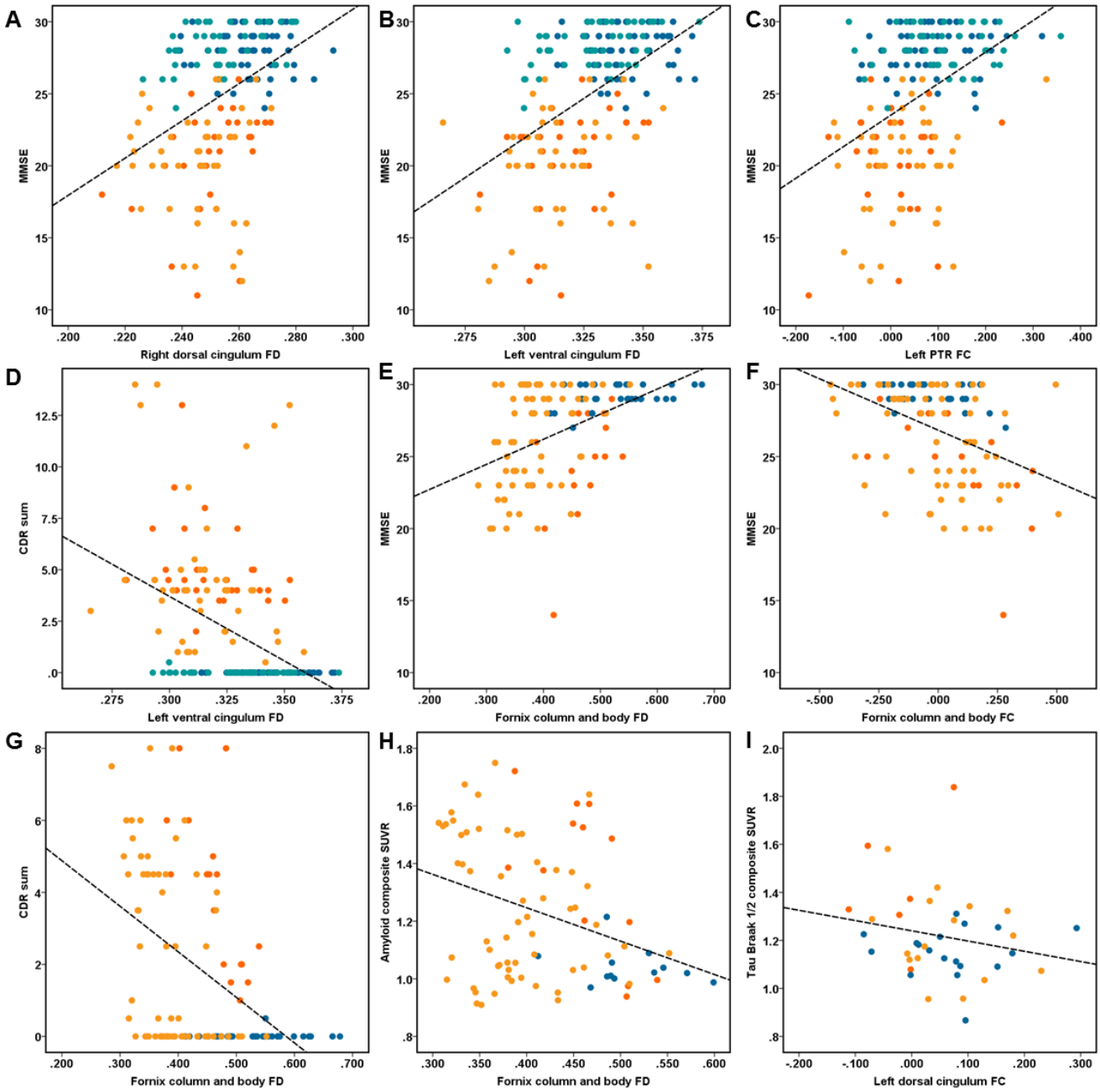

Figure 3

illustrates the association between fixel-based analysis metrics and clinical data.

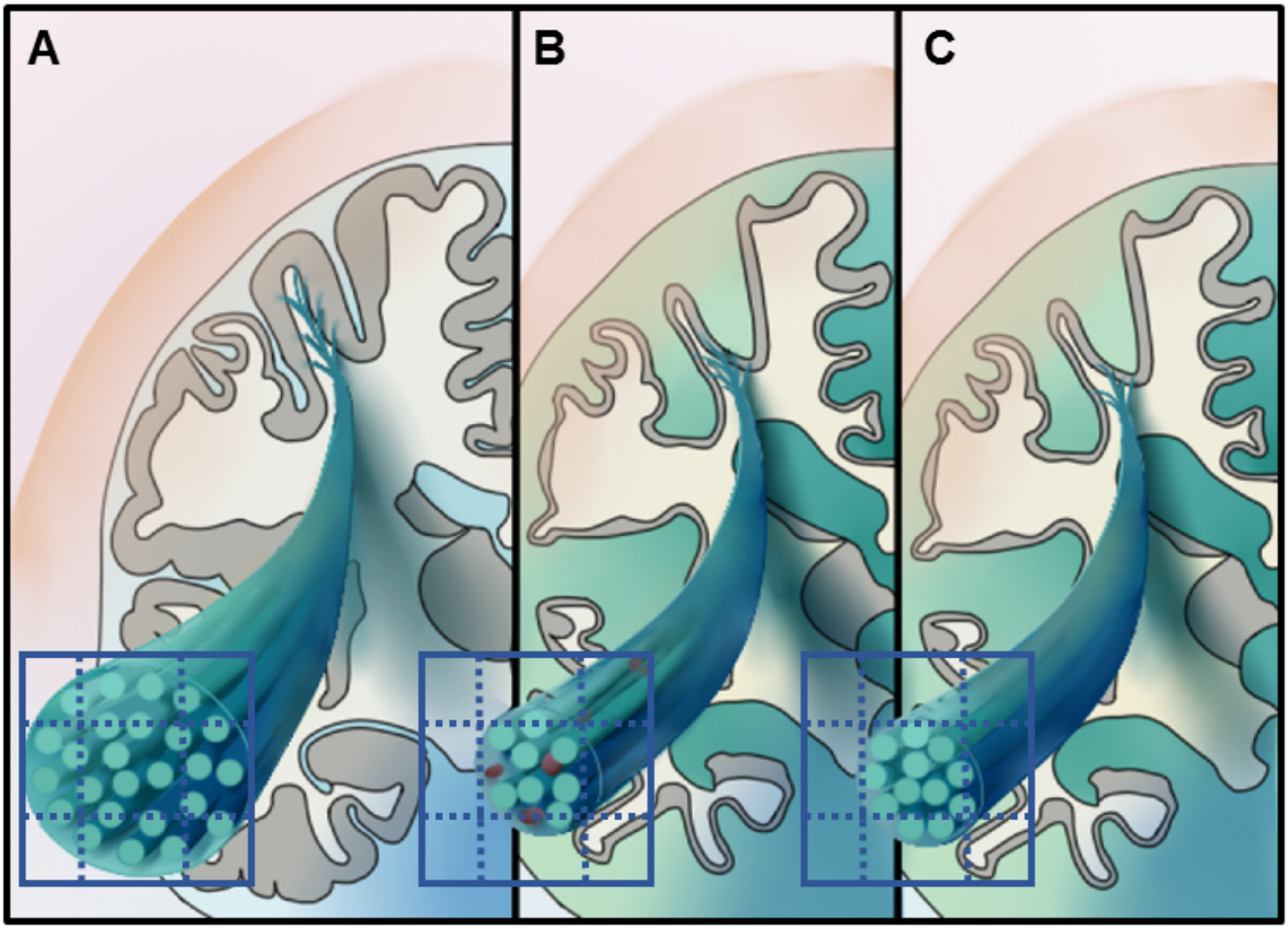

Figure 4

illustrates the hypothetical model of white matter pathological processes in early-onset Alzheimer's disease (EOAD) and late-onset Alzheimer's disease (LOAD).

Supplementary Files

This is a list of supplementary files associated with this preprint. Click to download.

- Supplementary.docx
- SupplementaryTables.docx